

Transport-Dependent Alterations of Membrane Properties of Mammalian Colon Measured Using Impedance Analysis

N.K. Wills†* and C. Clausen‡

†Department of Physiology, Yale University School of Medicine, New Haven, Connecticut 06437, and ‡Department of Physiology and Biophysics, Health Science Center, Stony Brook, New York 11794-8861

Summary. Direct current (DC) measurement methods have been commonly used to characterize the conductance properties of the mammalian colon. However, these methods provide no information concerning the effects of tissue morphology on the electrophysiological properties of this epithelium. For example, distribution of membrane resistances along narrow fluid-filled spaces such as the lateral intercellular spaces (LIS) or colonic crypts can influence DC measurements of apical and basolateral membrane properties. We used impedance analysis to determine the extent of such distributed resistance effects and to assess the conductance and capacitance properties of the colon. Because capacitance is proportional to membrane area, this method provides new information concerning membrane areas and specific ionic conductances for these membranes.

We measured transepithelial impedance under three conditions: (1) control conditions in which the epithelium was open-circuited and bathed on both sides with NaCl-HCO₃ Ringer's solutions, (2) amiloride conditions which were similar to control except that 100 μM amiloride was present in the mucosal bathing solution, and (3) mucosal NaCl-free conditions in which mucosal Na and Cl were replaced by potassium and sulfate or gluconate ("K⁺ Ringer's"). Three morphologically-based equivalent circuit models were used to evaluate the data: (1) a lumped model (which ignores LIS resistance), (2) a LIS distributed model (distributed basolateral membrane impedance) and (3) a crypt-distributed model (distributed apical membrane impedance). To estimate membrane impedances, an independent measurement of paracellular conductance (G_p) was incorporated in the analysis. Although distributed models yielded improved fits of the data, the distributed and lumped models produced similar estimates of membrane parameters. The predicted effects of distributed resistances on DC microelectrode measurements were largest for the LIS-distributed model. LIS-distributed effects would cause a 12–15% underestimate of membrane resistance ratio (R_a/R_b) for the control and amiloride conditions and a 34% underestimate for the "K⁺ Ringer's" condition. Distributed resistance effects arising from the crypts would produce a 1–2% overestimate of R_a/R_b .

Apical and basolateral membrane impedances differed in the three different experimental conditions. For control conditions, apical membrane capacitance averaged 21 μF/cm² and the mean apical membrane specific conductance (G_{a-norm}) was 0.17

mS/μF. The average basolateral membrane capacitance was 11 μF/cm² with a mean specific conductance (G_{b-norm}) of 1.27 mS/μF. G_{a-norm} was decreased by amiloride or "K⁺ Ringer's" to 0.07 mS/μF and 0.06 mS/μF, respectively. Basolateral conductance was also reduced by amiloride, whereas capacitance was unchanged ($G_{b-norm} = 0.97$ mS/μF). For the "K⁺ Ringer's" condition, both basolateral conductance and capacitance were greatly increased such that G_{b-norm} was not significantly different from the control condition.

Key Words impedance analysis · epithelium · colon · amiloride · equivalent circuit analysis

Introduction

The mammalian colon *in vivo* actively absorbs sodium and secretes potassium. In both the rabbit descending colon and the human descending colon, Na⁺ absorption is electrogenic and involves passive movement of this ion across the apical membrane through Na⁺ channels that can be blocked by the diuretic drug amiloride (Zeiske, Wills & Van Driessche, 1982; Wills, Alles, Sandle & Binder, 1984). Active extrusion of Na⁺ from the cell (and active uptake of potassium from the serosa) is accomplished by the Na-K ATPase in the basolateral membrane. In parallel to this Na⁺ transport system are two active transport systems for potassium: one absorptive and the other secretory (McCabe, Cooke & Sullivan, 1982; Wills & Biagi, 1982). The absorptive system includes active K⁺ uptake across the apical membrane and passive exit to the serosa via a large potassium conductance in the basolateral membrane (Wills, Lewis & Eaton, 1979; Wills, 1985). In contrast, the active step for K⁺ secretion is located at the basolateral membrane and (as indicated above) is mediated by the basolateral membrane Na-K ATPase. Exit across the apical membrane is passive and is thought to involve a conductive mechanism (Wills, 1985).

Previous studies have used direct current (DC)

* Present address: Department of Physiology and Biophysics, University of Texas Medical Branch, Galveston, TX 77550-2781.

equivalent circuit analysis in conjunction with microelectrode techniques to resolve the ionic conductance properties of the apical and basolateral membranes of the colon. In general, these studies have indicated that the colon is a "moderately" tight epithelium with comparable conductances for the paracellular and cellular pathways (Schultz, Frizzell & Nellans, 1977; Wills et al., 1979). Recent evidence by Welsh, Smith, Fromm and Frizzell (1982) indicates that the amiloride-sensitive Na^+ conductance is localized in the apical membrane of surface epithelial cells, i.e., the so-called absorptive cell type. In contrast, amiloride appeared to have virtually no effect on the apical membrane properties of crypt cells. The apical membrane of surface cells also demonstrated an additional (and equally large) conductance that is not sensitive to amiloride (Wills et al., 1979; Thompson, Suzuki & Schultz, 1982b; Welsh, Smith, Fromm & Frizzell, 1982). Recent evidence suggests that at least part of this conductance is due to potassium (Wills, 1985).

Unfortunately, DC methods for measuring membrane properties do not provide information concerning the influence of tissue morphology on membrane electrical properties. For example, microelectrode methods do not provide information concerning the areas of the apical and basolateral membranes. Consequently, it is not possible to resolve whether changes in membrane conductance are due to alterations in membrane area or reflect changes in the specific ionic conductances of the membrane (i.e., the number of conductive units per unit area of membrane). This limitation can be overcome by using DC methods in conjunction with frequency domain techniques which do provide estimates of membrane area. These estimates are obtained from measurements of membrane capacitance. Membrane capacitance is proportional to area and nearly all biological membranes exhibit a specific capacitance of approximately $1 \mu\text{F}/\text{cm}^2$ (Cole, 1972).

A second limitation of DC microelectrode techniques is the sensitivity of these methods to distributed resistance effects. Clausen, Lewis and Diamond (1979) and Boulpaep and Sackin (1980) have shown that membrane resistance ratios can be artificially decreased by distributed resistance effects when the series resistance of the lateral intercellular space (LIS) becomes comparable to the basolateral membrane resistance. Since DC analysis methods often rely on membrane resistance ratio measurements, such distributed resistance effects can result in errors, particularly underestimation of the true membrane resistance ratio, leading to an underestimation of apical membrane resistance. Indeed, on the basis of their microelectrode studies of the frog

skin, Nagel, Garcia-Diaz, and Essig (1983) hypothesized that these effects might be important in the interpretation of membrane resistance ratio measurements in the rabbit descending colon. They concluded that this artifact could explain the amiloride-insensitive apical membrane conductance reported in previous experiments.

In the present study we used impedance analysis methods to resolve this issue. First, we evaluated the extent of distributed resistance effects by comparing impedance results to the predictions of three equivalent circuit models. The models included a lumped model which was similar to that employed in our previous DC equivalent circuit analysis and two morphologically-based distributed models. Specifically, we asked the following questions: (1) Are distributed resistance effects large enough to influence DC microelectrode measurements of membrane resistance ratios? (2) What are the effects of Na^+ transport rate on apical and basolateral membrane properties? and (3) What role does luminal potassium play in determining membrane electrical properties?

Materials and Methods

ANIMALS AND CHAMBER DESIGN

New Zealand white rabbits (2–3 kg) were sacrificed with an i.v. injection of sodium pentobarbital. A 10–15 cm segment of descending colon was removed, opened as a flat sheet and rinsed free of contents. The epithelium was then removed by glass slide dissection using the method of Frizzell, Koch and Schultz (1976). The isolated epithelium was then mounted vertically in an Ussing chamber which was designed to eliminate edge damage (exposed tissue area: 2 cm^2). The bathing solutions were maintained at 37°C and were continuously stirred and bubbled with a mixture of 95% O_2 and 5% CO_2 .

SOLUTIONS

The tissue was normally bathed with a NaCl - NaHCO_3 Ringer's solution with the following composition (in mM): 136 Na^+ , 7 K^+ , 121 Cl^- , 2 Ca^{2+} , 1.2 Mg^{2+} , 25 HCO_3^- , $1.2 \text{ H}_2\text{PO}_4^-$, 1.2 SO_4^{2-} and 11 mM D-glucose . For gluconate or potassium Ringer's, chloride and/or sodium were replaced by gluconate and/or potassium, respectively. The sulfate Ringer's solution was similar to the above solutions except no chloride was present, SO_4^{2-} was 59 mM, and Ca^{2+} was 10 mM. In addition, the solution contained 20 mM MeSO_4 and 120 mM sucrose (see also Wills et al., 1979). Amiloride (a generous gift of Merck, Sharpe, and Dohme Corp., Rahway, N.J.) was prepared as a concentrated stock solution in distilled water and was added in aliquots to a final concentration of $100 \mu\text{M}$. Nystatin (Sigma Chemical Co., St. Louis, Mo.) was prepared as a 5-mg/ml stock solution (2,900 units/ml) in methanol.

TRANSEPITHELIAL ELECTRICAL MEASUREMENTS

Transepithelial voltage and current-passing electrodes were Ag-AgCl wires or (in the case of Cl^{-1} -free experiments) 1 M NaCl agar bridges led to half cells which consisted of Ag-AgCl electrodes immersed in 3 M KCl solutions. Voltage electrodes were mounted immediately adjacent to the preparation and led to a low-noise, high-impedance, differential amplifier (model 113, Princeton Applied Research, Princeton, N.J.). Current electrodes were situated at the rear of each chamber. The serosal current electrode was grounded and constant current was generated using a calibrated 1 or 10 M Ω carbon series resistor. For DC measurements of transepithelial parameters, procedures were identical to those described by Wills et al. (1979). Transepithelial resistance was calculated from (R_T) from the voltage response to a 500-msec current pulse ($50 \mu\text{A}/\text{cm}^2$). Short-circuit current (I_{sc}) was calculated from the transepithelial potential (V_T) and R_T using Ohm's law. All measurements were corrected for the effects of series resistance of the bathing solutions, electrode asymmetry and diffusion potentials.

TRANSEPITHELIAL IMPEDANCE ANALYSIS

Transepithelial impedance was measured using the method of Clausen and Fernandez (1981) as detailed in Clausen, Reinach, and Marcus (1986). Briefly, a wide-band pseudo-random binary noise signal was generated digitally and converted to a constant transepithelial current of $14 \mu\text{A}/\text{cm}^2$ (peak-to-peak). The resulting transepithelial voltage response was amplified, filtered by an anti-aliasing filter, digitized, and recorded by computer. The impedance was calculated by dividing the cross-spectral density of the voltage and the current by the power-spectral density of the applied current. Two digitizing bandwidths were used to provide good resolution at low and high frequencies. In addition, signal averaging was employed to increase the signal-to-noise ratio. Total data acquisition time was less than 5 sec per run. Each run resulted in approximately 400 data points linearly spaced in frequency from 2.2 to 860 Hz, and an equal number of data points linearly spaced in frequency from 22 Hz to 8.6 kHz. These data were subsequently merged and reduced to 100 data points (actually 200 numbers since each data point consists of a phase angle and impedance magnitude measurement) logarithmically spaced in frequency from 2.2 Hz to 8.6 kHz.

The impedance was represented as Bode plots, which plot phase angle and log impedance against frequency. The data were then fitted by morphologically-based equivalent circuit models composed of resistors (representing membrane ionic conductances) and capacitors (representing membrane capacitances which are proportional to membrane area). Fitting of the data was accomplished using a nonlinear least squares curve fitting algorithm. After each curve fit, the Hamilton R-factor was computed as an objective measure of fit. The R-factor indicates the average per cent misfit between the model and the data. R-ratio tests (see Results) were used to compare the quality of fits generated by the different models. In addition to the R-factor, standard deviations were estimated for each parameter. It should be noted that the estimates of the parameter standard deviations are computed from a linearization of the model about the best-fit parameter set (see Hamilton, 1964). They do not reflect a true confidence interval for each parameter due to the nonlinear dependence of the impedance on each parameter (see Valdiosera, Clausen & Eisenberg, 1974). Nonetheless, a large standard devi-

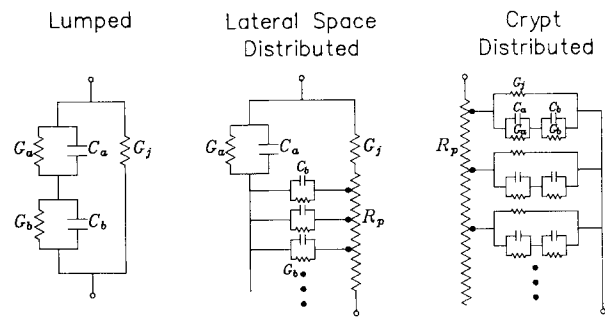


Fig. 1. Equivalent circuit models used to represent transepithelial impedance. *Left panel:* Lumped model. C_a and G_a are apical membrane capacitance and conductance, C_b and G_b are basolateral membrane capacitance and conductance, and G_j is paracellular (tight junctional) conductance. *Middle panel:* LIS-distributed model. Distributed resistance effects could arise when the series pathway resistance (R_p) of the lateral intercellular space (LIS) becomes comparable to the basolateral membrane impedance. *Right panel:* Crypt-distributed model. The colon is invaginated with crypts. Distributed resistance effects could arise when the series path resistance (R_p) of the crypt lumen becomes comparable to the apical membrane impedance

ation estimate indicates that a parameter is poorly determined. For this reason, data were excluded from further analysis if any parameter had a standard deviation which exceeded the best-fit value for that parameter by more than 10%.

Data acquisition and computations were performed using a PDP 11/34A computer system. For further details of data acquisition, curve fitting, and statistical computations, see Clausen et al. (1979, 1986).

EQUIVALENT CIRCUIT MODELS

The simplest circuit model appropriate for representing the transepithelial impedance, the lumped model, is shown on the left side of Fig. 1. The apical membrane is represented by a parallel resistor-capacitor (RC) circuit where the resistor corresponds to the membrane's ionic conductance (G_a) and the capacitor corresponds to the membrane's capacitance (C_a). (Recall that nearly all biological membranes exhibit a specific capacitance of $\sim 1 \mu\text{F}/\text{cm}^2$). The basolateral membrane is similarly represented by a lumped RC circuit, where the circuit elements (G_b and C_b) have similar meanings. The ionic conductance of the paracellular pathway is represented by a parallel resistor, R_j ($= 1/G_j$). Since the cross-sectional area of the junctions is negligible compared to the apical and basolateral membrane areas, the capacitance of the junctions can be ignored (Clausen et al., 1979).

The transepithelial impedance of the lumped model is given by

$$Z_T(j\omega) = (Y_a + Y_b)/[Y_a Y_b + G_j(Y_a + Y_b)] \quad (1)$$

where the respective membrane admittances are: $Y_a = G_a + j\omega C_a$ and $Y_b = G_b + j\omega C_b$. ω is the angular frequency ($2\pi f$, where f is frequency in Hz) and j is $\sqrt{-1}$.

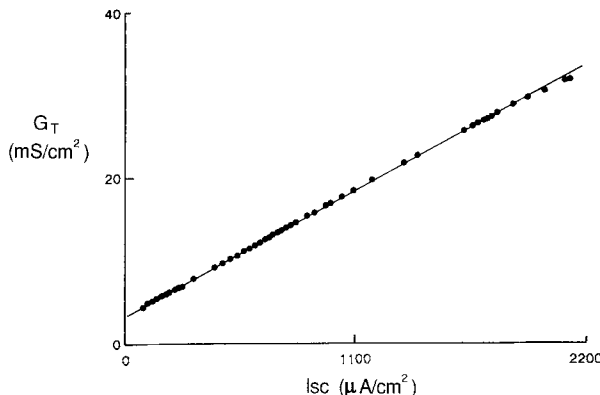


Fig. 2. Representative experiment showing transepithelial conductance (G_T) and short-circuit current (I_{sc}) after the addition of nystatin to the mucosal bath. The epithelium is bathed on the serosal side with NaCl Ringer's solution and with K^+ Ringer's solution on the mucosa (see Materials and Methods). A linear regression of these data yielded a correlation coefficient of 0.99 and a conductance intercept (G_s) of 3.23 mS/cm^2 . G_s is a measure of paracellular shunt conductance (Wills et al., 1979)

DISTRIBUTED EFFECTS

The lumped model presented above ignores effects resulting from series resistances arising from narrow fluid-filled spaces. We were concerned that the resistance of the lateral intercellular spaces and/or the resistance of the colonic crypts might become comparable to membrane impedances, especially at high frequencies. Therefore, to further investigate this possibility, we used two equivalent-circuit models that more closely represented the observed morphology of the epithelium.

The first model investigated is a modification of the lumped model which takes into account the LIS resistance (path resistance, R_p) by treating the basolateral membrane and lateral spaces as a distributed circuit (see Fig. 1, lateral space distributed model). The transepithelial impedance of this LIS-distributed model is given by

$$Z_T = \frac{Y_a + Y_b + G_j[Y_a Y_b / (Y_b R_p) + 2(1 - \operatorname{sech} \sqrt{Y_b / G_b})]}{Y_a Y_b + G_j(Y_a + Y_b)} \quad (2)$$

where $Y_b = \sqrt{Y_b R_p} \operatorname{tanh} \sqrt{Y_b R_p}$.

Distributed resistance effects could also arise from the resistance of deep crypts adjacent to the apical membrane. Typically these crypts have a luminal diameter of approximately $20 \mu\text{m}$ and are $400\text{--}500 \mu\text{m}$ in length (N.K. Wills and B. Biagi, *unpublished observations*). Conceivably crypts of this dimension could offer a significant luminal resistance which would distribute along the apical surface of the epithelium. The simplest model that explicitly considers the resistance of the crypts is seen on the right side of Fig. 1. The impedance of this crypt-distributed model is given by:

$$Z_T(j\omega) = \sqrt{R_p Z} \operatorname{coth} \sqrt{R_p / Z} \quad (3)$$

where Z equals the previous lumped impedance shown in Eq. (1).

Note that Eqs. (1)–(3) do not show the additive series resistance (R_{se}), defined as the resistance of the bathing solution between the voltage electrodes and the epithelial surface.

DERIVATION OF MEMBRANE CIRCUIT PARAMETERS

From transepithelial impedance data alone, it is impossible to estimate membrane parameters directly from the above equivalent circuits without an independent measurement of at least one circuit parameter. Unlike previous studies of the corneal epithelium (Clausen et al., 1986) and mammalian urinary bladder (Clausen et al., 1979), we chose not to use membrane resistance ratios as the independent parameter. The colon contains more than one cell type, and the cells are difficult to impale. The latter problem is significant since the colon survives only for a few hours *in vitro*. For these reasons, we chose instead to use estimates of the paracellular resistance, R_s , obtained using the method of Wills et al. (1979; *see also* Wills, 1981). Briefly, this method consists of using the polyene antibiotic nystatin to increase the apical membrane conductance (G_a) to small monovalent ions. The mucosal bathing solution is first replaced by a K_2SO_4 or K gluconate Ringer's solution that has a K^+ activity approximately equal to the intracellular potassium activity (Wills et al., 1979; Wills, 1985). Nystatin (39 unit/ml) is then added to the mucosal bath. The transepithelial conductance (G_T) and I_{sc} increased linearly as follows:

$$G_T = I_{sc}/E_b + G_s \quad (4)$$

where E_b is the emf of the basolateral membrane. R_s is estimated from the inverse intercept of this function ($1/G_s$). The data were fitted incorporating this value of R_s to obtain estimates of G_a , G_b , C_a , C_b , and R_p .

Results

Transepithelial impedance was measured in 13 colons from 13 animals. To estimate individual membrane parameters, the data were fitted to the three morphologically-based equivalent circuit models described above. The analysis incorporated R_s values determined for each tissue using the nystatin method (*see above*). The average value of R_s was $677 \pm 80 \Omega \cdot \text{cm}^2$, in good agreement with our previous studies (Wills et al., 1979). An example of a typical nystatin experiment is given in Fig. 2.

Figure 3(A and B) shows the results of impedance measurements for a typical experiment when the tissue was bathed on both sides with NaCl-HCO₃ Ringer's solution under open-circuit conditions (i.e., "control" conditions). Inspection of Fig. 3A reveals that the magnitude of the impedance decreased at frequencies above 10 Hz and showed a plateau at frequencies above 1 kHz. The plateau level at high frequencies reflects the series resistance (R_{se}) of the bathing solutions, whereas the low frequency magnitude approaches the DC resistance of the preparation (R_T). The results of fitting the

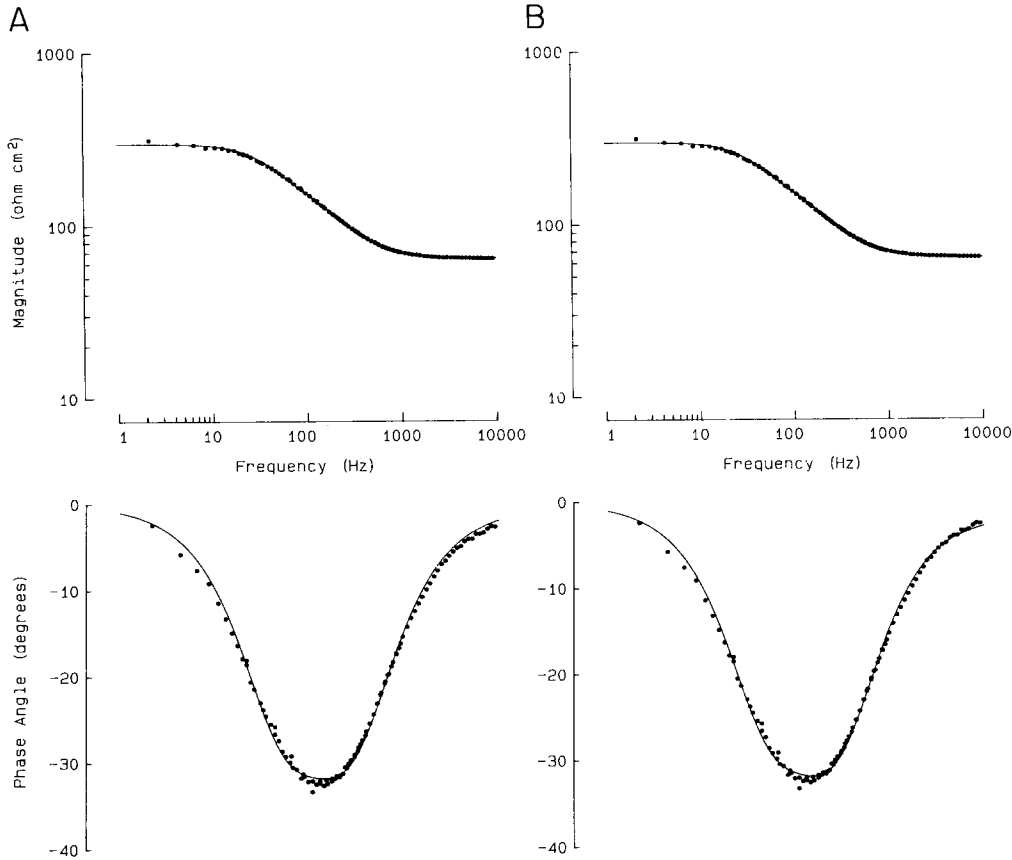


Fig. 3. (A) Representative results from a single experiment showing a Bode plot of impedance phase angle and magnitude data. Symbols are measured data, solid lines are the fit by the lumped model. The results of the fit were as follows: $G_a = 3.99 \text{ mS/cm}^2$, $C_a = 21.8 \mu\text{F/cm}^2$, $G_{bl} = 17.7 \text{ mS/cm}^2$, $C_{bl} = 15.4 \mu\text{F/cm}^2$, $R_{se} = 64.6 \Omega \text{ cm}^2$, R-factor = 1.7%. (B) The same data fitted by the LIS-distributed model. A slight improvement in fit was obtained (R-factor = 1.5%). $G_a = 4.03 \text{ mS/cm}^2$, $C_a = 22.3 \mu\text{F/cm}^2$, $G_{bl} = 17.3 \text{ mS/cm}^2$, $C_{bl} = 15.6 \mu\text{F/cm}^2$, $R_p = 10 \Omega \text{ cm}^2$, $R_{se} = 61.8 \Omega \text{ cm}^2$. The crypt-distributed model produced an essentially identical improvement in fit. (R-factor = 1.5%, $G_a = 4.03 \text{ mS/cm}^2$, $C_a = 22.4 \mu\text{F/cm}^2$, $G_{bl} = 17.0 \text{ mS/cm}^2$, $C_{bl} = 15.6 \mu\text{F/cm}^2$, $R_p = 9.2 \Omega \text{ cm}^2$, $R_{se} = 61.8 \Omega \text{ cm}^2$)

data by the lumped model are shown by the smooth curve. As indicated by this illustration, a reasonable fit of the data was obtained using the lumped model, although improved fits were obtained using the LIS and crypt-distributed models (see Fig. 3B).

The membrane parameters estimated by the three different models are summarized in Table 1. Estimates of membrane conductance and capacitance showed little variation between models. Apical membrane conductance (G_a) averaged $3.5 \pm 0.06 \text{ mS/cm}^2$ for the three models, whereas apical membrane capacitance (C_a) averaged $21.3 \pm 0.6 \mu\text{F/cm}^2$. Values for the crypt-distributed model were 8% larger than C_a values estimated from the lumped or LIS-distributed models. The mean G_b estimate was $13.1 \pm 0.4 \text{ mS/cm}^2$, while the mean C_b was $10.6 \pm 0.4 \mu\text{F/cm}^2$. As indicated in Table 1 small differences between the lumped and distributed models were found for some of these parameters. While these differences sometimes reached statistical sig-

nificance, they were not systematically related to the choice of model.

Table 1 also includes a summary of residual errors (see “R-factor”) for the various models. As mentioned above, the R-factor provides an objective measure of the average relative discrepancy between the data and the model-predicted impedance such that smaller R-factors indicate an improved quality of the curve fit. Both the LIS and crypt-distributed models showed significantly lower R-factor values than the lumped model, indicating superior fits to the data. However, this result is expected since the distributed models each possess an additional adjustable parameter and the inclusion of an additional variable (even a meaningless one) is expected to improve the fit to the data. Therefore, it was necessary to verify that the variance of the data was low enough to permit the determination of the additional parameter. To assess this problem, we used the R-ratio test (a modified F test; see Clausen

Table 1. Comparison of lumped and distributed models

Model	G_a (mS/cm ²)	C_a (μ F/cm ²)	G_b (mS/cm ²)	C_b (μ F/cm ²)	R-factor (%)
Lumped	3.45 ± 0.37	20.7 ± 1.7	13.9 ± 1.0	9.8 ± 0.7	2.6 ± 0.3
LIS-distributed	3.53 ± 0.38	20.7 ± 2.0	12.7 ± 1.2	10.9 ± 0.9	1.8 ± 0.2
P^a	<0.05	NS	NS	<0.05	
Crypt-distributed	3.65 ± 0.43	22.4 ± 2.0	12.8 ± 1.0	11.1 ± 1.0	1.6 ± 0.1
P^a	NS	<0.001	<0.01	NS	

n = 12. NaCl-HCO₃ Ringer's solution, both sides.

^a Compared to lumped model, paired *t*-test.

Table 2. Distributed resistances and membrane conductances normalized for membrane capacitance

Model	$G_{a\text{-norm}}$ (mS/ μ F)	$G_{b\text{-norm}}$ (mS/ μ F)	R_p ($\Omega \cdot \text{cm}^2$)	R_a/R_b^*
Lumped	0.17 ± 0.01	1.45 ± 0.11	—	5 ± 0.4
LIS-distributed	0.18 ± 0.03	1.16 ± 0.07	28 ± 8	4 ± 0.5
P^{\dagger}	NS	<0.05	—	NS
Crypt-distributed	0.16 ± 0.01	1.19 ± 0.08	22 ± 2	4 ± 0.4
P^{\dagger}	NS	<0.01	—	NS

* Calculated as G_b/G_a from membrane conductances normalized to 1 cm² nominal tissue area, i.e., G_a (mS/cm²) and G_b (mS/cm²).

[†] Compared to lumped model, paired *t*-test.

Table 3. Effects of amiloride or mucosal NaCl replacement (K⁺ gluconate or K₂SO₄ Ringer's) on transepithelial electrical parameters

	V_T (mV)	I_{sc} (μ A/cm ²)	R_T ($\Omega \cdot \text{cm}^2$)
Control	-30 ± 5	112 ± 26	283 ± 25
Amiloride	0 ± 2 ^a	-3 ± 4 ^a	426 ± 48 ^a
<i>n</i> = 7			
Control	-31 ± 3	95 ± 15	356 ± 44
K gluconate or K ₂ SO ₄ mucosa	-28 ± 4	56 ± 13 ^a	480 ± 41 ^a
<i>n</i> = 13			

^a *P* < 0.05.

et al., 1979) to determine whether the addition of another parameter was justified. In every case, the results of this analysis were highly significant for both distributed models ($P \ll 0.0005$), indicating that the determination of the additional distributed parameter (R_p) was statistically warranted.

In summary of Table 1, improved fits were found for the LIS and crypt-distributed models. Overall these models yielded estimates of membrane parameters which were similar to those obtained using the more simple lumped model. Average results across models were 3.5 ± 0.1 mS/cm² for apical membrane conductance (G_a) and 13.1 ± 0.4 mS/cm² for G_b . Average membrane capacitances (C_a and C_b) were 21.3 ± 0.6 μ F/cm² and 10.6 ± 0.4 μ F/cm² for the apical and basolateral membranes, respectively.

Table 2 contains the data from the same experiments, summarizing distributed resistance parameters (for the LIS and crypt-distributed models), membrane resistance ratios, and specific membrane conductances (i.e., conductances normalized for membrane capacitance; $G_{a\text{-norm}} = G_a/C_a$ and $G_{b\text{-norm}} = G_b/C_b$). Beginning with distributed resistances (R_p), the LIS-distributed model estimated the LIS resistance as $28 \Omega \cdot \text{cm}^2$, whereas the crypt-distributed model estimated the crypt luminal resistance as $22 \Omega \cdot \text{cm}^2$. Because the LIS and crypt-distributed models attribute all distributed resistance to a

Table 4. Effects of amiloride on the impedance properties of the rabbit descending colon

Condition	Model	G_a (mS/cm ²)	C_a (μ F/cm ²)	G_b (mS/cm ²)	C_b (μ F/cm ²)	R-factor (%)
Control	Lumped	3.5 ± 0.4	23 ± 2	16 ± 1	11 ± 1	3.2 ± 0.4
	LIS-distributed	3.6 ± 0.4	24 ± 2	15 ± 1	13 ± 1	2.0 ± 0.4
	Crypt-distributed	3.8 ± 0.5	25 ± 2	14 ± 1	13 ± 1	1.8 ± 0.1
Amiloride (10 ⁻⁴ M mucosa)	Lumped	1.6 ± 0.3 ^a	20 ± 2 ^a	13 ± 1 ^a	12 ± 1 ^a	3.2 ± 0.4
	LIS-distributed	1.6 ± 0.4 ^a	21 ± 2 ^a	12 ± 1 ^a	13 ± 1	2.2 ± 0.2
	Crypt-distributed	1.6 ± 0.3 ^a	22 ± 2 ^a	12 ± 1 ^a	14 ± 1	1.9 ± 0.2

n = 7.^a *P* < 0.05 compared to control, paired *t* test.

single parameter (R_p), this value represents the maximal estimate for the LIS resistance or crypt resistance, respectively.

The specific conductance of the apical membrane was not significantly different between the three models and averaged 0.17 ± 0.005 mS/ μ F. In contrast, distributed models gave slightly lower estimates of $G_{b\text{-norm}}$ than the lumped model. $G_{b\text{-norm}}$ for the lumped model was 1.45 mS/ μ F, whereas the distributed models gave a mean estimate of 1.18 ± 0.02 mS/ μ F. Membrane resistance ratios (R_a/R_b) shown in Table 2 were calculated as G_b/G_a from membrane conductances (normalized to 1 cm² tissue area). However, the ratio of $G_{b\text{-norm}}$ to $G_{a\text{-norm}}$ (i.e., $R_{a\text{-norm}}/R_{b\text{-norm}}$) averaged 7 ± 0.7 for the three models, indicating that the basolateral membrane is much more conductive than the apical membrane.

AMILORIDE EFFECTS

Table 3 summarizes DC measurements of transepithelial electrical parameters (V_T , R_T , and I_{sc}) before and after addition of 10^{-4} M amiloride to the mucosal solution or replacement of mucosal Na^+ and Cl^- by potassium sulfate or potassium gluconate. In agreement with previous studies (Frizzell et al., 1976; Wills et al., 1979), addition of 50–100 μ M amiloride to the mucosal bath increased transepithelial resistance and essentially abolished the short-circuit current and transepithelial potential.

Figure 4 summarizes the results of seven experiments and illustrates the relationship between R_T and V_T (see Lewis & Wills, 1982). In this representation the R_T intercept reflects the sum of the paracellular conductance (G_s) and the conductance of amiloride-insensitive cells (c.f. Wills et al., 1979). The slope of the plot reflects the emf of the amiloride-

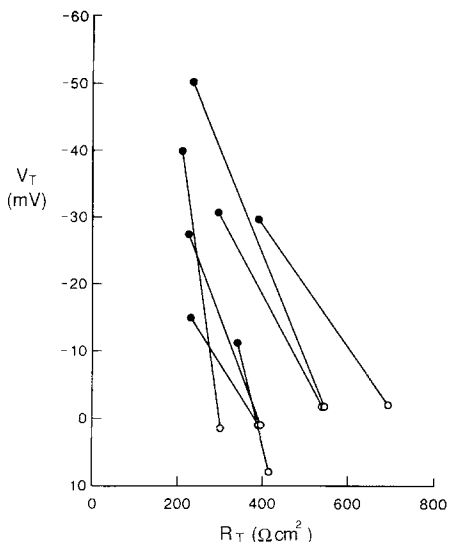


Fig. 4. Transepithelial voltage (V_T) and resistance (R_T) measurements before (filled circles) and after (open circles) mucosal addition of 10^{-4} M amiloride. For description, see text

sensitive pathway (E_{Na}). As indicated by this figure, there was considerable variability in R_s and E_{Na} . This point will be discussed in more detail below.

Impedance data for the amiloride condition were reasonably well fitted by the lumped model, similar to the control condition shown previously in Fig. 3. As with the control condition, improved fits were found with both the LIS-distributed model and crypt model. The results for pooled experiments are summarized in Table 4. The amiloride concentration in these experiments was 100 μ M. Preliminary experiments using lower dosages (50 μ M) gave similar results. As in the case of the control condition, the three models were in general agreement con-

Table 5. Effects of amiloride on membrane conductances normalized for membrane capacitance

Condition Model	$G_{a\text{-norm}}$ (mS/ μ F)	$G_{b\text{-norm}}$ (mS/ μ F)	R_p ($\Omega \cdot \text{cm}^2$)	R_a/R_b	α	Mean % difference
Control						
Lumped	0.16 \pm 0.02	1.46 \pm 0.10	—	4.7 \pm 0.3	—	—
LIS-distributed	0.15 \pm 0.02	1.19 \pm 0.06	44 \pm 14	4.3 \pm 0.3	3.7 \pm 0.4	-15 \pm 4
Crypt-distributed	0.16 \pm 0.02	1.12 \pm 0.05	28 \pm 6	4.0 \pm 0.3	4.1 \pm 0.3	1 \pm 0.1
Amiloride (10^{-4} M mucosa)						
Lumped	0.08 \pm 0.01 ^a	1.08 \pm 0.08 ^a	—	9.9 \pm 1.8 ^a	—	—
LIS-distributed	0.07 \pm 0.01 ^a	0.95 \pm 0.08 ^a	45 \pm 5	10.0 \pm 1.9 ^a	8.6 \pm 1.4	-12 \pm 3
Crypt-distributed	0.07 \pm 0.01 ^a	0.88 \pm 0.08 ^a	28 \pm 5	9.1 \pm 1.6 ^a	9.2 \pm 1.6	1 \pm 0.3

n = 7.^a *P* < 0.05 compared to control.

cerning membrane parameter estimates. Amiloride addition significantly decreased G_a , G_b and C_a , whereas C_b was unchanged. The mean decreases (averaged over the three models) for G_a , G_b , and C_a were 56 \pm 1%, 13 \pm 1% and 18 \pm 2%, respectively.

Specific membrane conductances are presented in Table 5. The mean values of $G_{a\text{-norm}}$ and $G_{b\text{-norm}}$ for the control condition were not significantly different than those in Table 2. For the amiloride condition, $G_{a\text{-norm}}$ and $G_{b\text{-norm}}$ averaged 0.07 \pm 0.003 mS/ μ F and 0.97 \pm 0.06 mS/ μ F. This constitutes an average decrease of 53 \pm 2% in apical membrane specific conductance and a 23 \pm 2% decrease in basolateral membrane specific conductance.

Table 5 also contains membrane resistance ratios (R_a/R_b) calculated from the conductance data in Table 4 (i.e., G_b/G_a ; conductance values not normalized for membrane capacitance). These values averaged 4.3 \pm 0.2. In order to estimate the relative specific ionic conductances of the two membranes, we next computed membrane resistance ratios from membrane conductances normalized for capacitance. $R_{a\text{-norm}}/R_{b\text{-norm}}$ averaged 16 \pm 3, 18 \pm 5 and 14 \pm 2 for the lumped, distributed and crypt models, respectively. Therefore, after amiloride, the specific ionic conductance of the apical membrane decreased by twofold compared to the basolateral membrane conductance.

EFFECTS OF DISTRIBUTED RESISTANCES ON DC MEASUREMENTS OF R_a/R_b

Using impedance-derived estimates of R_a , R_b and R_p , we also calculated the "apparent" membrane resistance ratio, α , expected from DC microelectrode measurements for the LIS and crypt-distributed models. For the LIS-distributed model

$$\alpha = R_a/R'_b \quad (5)$$

where

$$R'_b = \sqrt{R_b R_p} \coth \sqrt{R_p/R_b} \quad (6)$$

and R_p is LIS resistance.

When $R_p/R_b < 0.15$, the equation can be simplified to

$$R'_b = R_b + \frac{1}{3}R_p. \quad (7)$$

(Note that the above approximation for R'_b is accurate within >98.5% when $R_p/R_b < 1$.)

Similarly, for the crypt model

$$\alpha = R'_a/R_b$$

where $R'_a = \sqrt{R_a R_p} \coth \sqrt{R_p/R_a}$ and R_p is crypt lumen resistance. Again, when $R_p/R_a < 0.15$, this relationship reduces to

$$R'_a = R_a + \frac{1}{3}R_p.$$

The mean percent difference between α and R_a/R_b values are presented in Table 5. For the LIS-distributed model, distributed resistance effects are expected to cause a 12–15% underestimate of R_a/R_b when this value is measured by DC microelectrode techniques. Distributed resistances along the crypt, in contrast, produce a 1% overestimate of this value. Therefore, distributed resistance effects on microelectrode measurements are minor for these conditions.

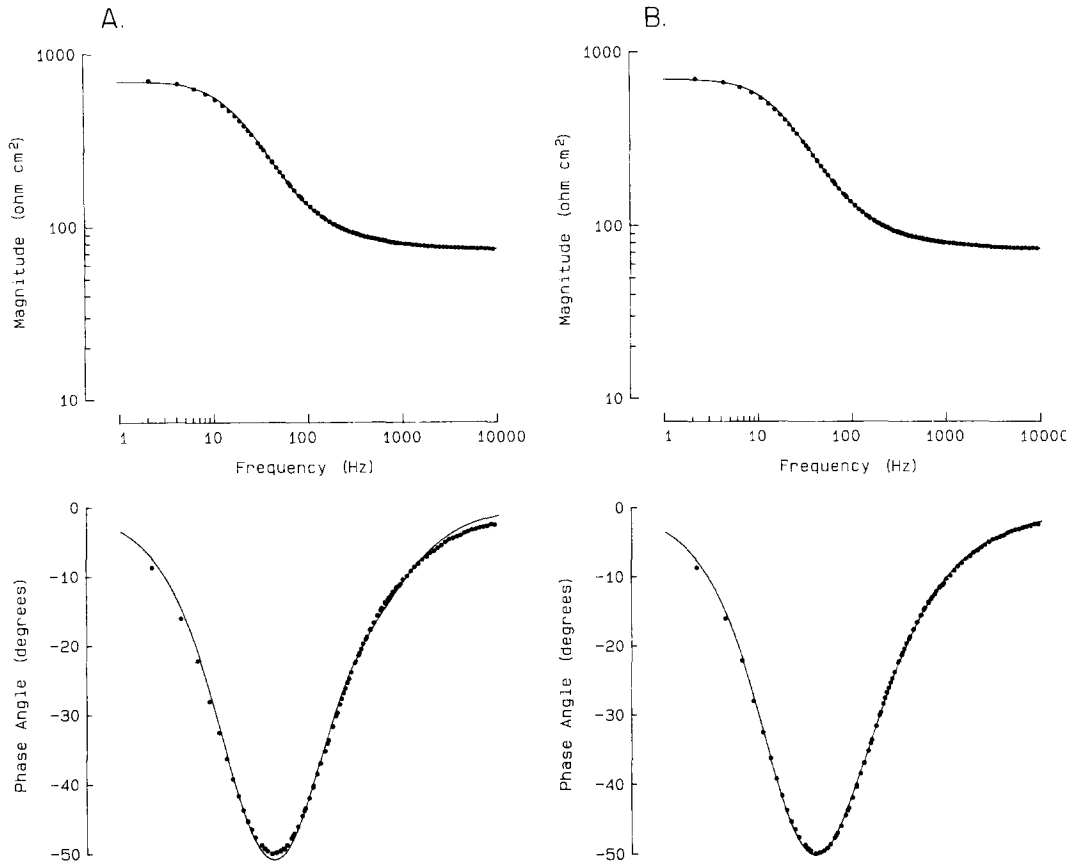


Fig. 5. Impedance from a single experiment showing the effects of mucosal replacement of Na^+ and Cl^- by potassium and gluconate. (A) Fit of the data by the lumped model. (R-factor = 1.5%, $G_a = 0.61 \text{ mS/cm}^2$, $C_a = 17.7 \mu\text{F/cm}^2$, $G_{bl} = 72.5 \text{ mS/cm}^2$, $C_{bl} = 23.9 \mu\text{F/cm}^2$, $R_{se} = 74.0 \Omega \text{ cm}^2$.) (B) The same data fitted by the LIS-distributed model. An improved fit was obtained. (R-factor = 0.7%, $G_a = 0.94 \text{ mS/cm}^2$, $C_a = 18.6 \mu\text{F/cm}^2$, $G_{bl} = 86.0 \text{ mS/cm}^2$, $C_{bl} = 88.9 \mu\text{F/cm}^2$, $R_p = 38.0 \Omega \text{ cm}^2$, $R_{se} = 72.0 \Omega \text{ cm}^2$.) The crypt-distributed model produced a similar improvement in fit (R-factor = 1.0%, $G_a = 0.60 \text{ mS/cm}^2$, $C_a = 18.0 \mu\text{F/cm}^2$, $G_{bl} = 74.0 \text{ mS/cm}^2$, $C_{bl} = 42.0 \mu\text{F/cm}^2$, $R_p = 22.0 \Omega \text{ cm}^2$, $R_{se} = 70.0 \Omega \text{ cm}^2$).

EFFECTS OF MUCOSAL POTASSIUM GLUCONATE AND POTASSIUM SULFATE RINGER'S SOLUTIONS (Na AND Cl REPLACEMENT)

In order to further assess the extent of distributed resistance effects, we next removed mucosal Na^+ and Cl^- and replaced them with potassium sulfate or potassium gluconate ("K⁺ Ringer's"). The results of sulfate and gluconate were similar and have been combined. As shown in Table 3 this procedure, like amiloride, increased transepithelial resistance. Unlike amiloride, I_{sc} was reduced but not abolished. V_T was not significantly affected.

Figure 5(A and B) is an example of a Bode plot of transepithelial impedance for the mucosal "K Ringer's" condition. As for the other experimental conditions, distributed models produced better fits to the data as can be seen by comparing the smooth

curve for the phase angle data in Fig. 5A (lumped model) to that in Fig. 5B (LIS-distributed model).

A summary of membrane conductances and capacitances and R-factors for the three models for this condition are given in Table 6. In comparison to paired control values (NaCl Ringer's, *see* Table 1), all membrane parameters were significantly altered by mucosal "K Ringer's." No significant differences were noted between lumped and distributed model estimates for apical membrane conductance or capacitance (G_a and C_a). Averaged over models, G_a and C_a were reduced by $72 \pm 0.5\%$ and $19 \pm 2\%$, respectively. In contrast, G_b and C_b were both increased. The magnitude of the increase varied slightly across models, but averaged $163 \pm 12\%$ for G_b and $207 \pm 92\%$ for C_b .

Table 7 presents membrane specific conductances, distributed resistance (R_p) values, and com-

Table 6. Effects of "K-Ringer's" solution^a on membrane impedance

Model	G_a (mS/cm ²)	C_a (μ F/cm ²)	G_b (mS/cm ²)	C_b (μ F/cm ²)	R-factor (%)
Lumped	0.7 ± 0.2	16 ± 1	40 ± 5	18 ± 2	2.9 ± 0.4
LIS-distributed	0.9 ± 0.2	17 ± 2	32 ± 6	53 ± 11	1.4 ± 0.2
P^b	NS	NS	<0.05	<0.01	
Crypt-distributed	0.8 ± 0.2	19 ± 2	32 ± 6	28 ± 04	1.7 ± 0.2
P^b	NS	NS	<0.05	<0.01	

n = 12.^a Mucosal K₂SO₄ or potassium gluconate Ringer's solution. Paired control measurements (NaCl Ringer's mucosal solution) are given in Table 1.^b Compared to lumped model, paired *t* test.**Table 7.** Effects of "K-Ringer's" mucosal solution on membrane conductances normalized to membrane capacitance

Model	G_a (mS/ μ F)	G_b (mS/ μ F)	R_p ($\Omega \cdot \text{cm}^2$)	R_a/R_b	α	Mean % difference
Lumped	0.06 ± 0.01	2.22 ± 0.19	—	63 ± 13	—	—
LIS-distributed	0.06 ± 0.01	1.19 ± 0.52	64 ± 8	44 ± 11	26 ± 6	-34 ± 4
P^*	NS	NS				
Crypt-distributed	0.06 ± 0.01	1.25 ± 0.17	80 ± 12	45 ± 11	46 ± 11	2 ± 0.7
P^*	NS	<0.001				

n = 12.^{*} Compared to lumped model, paired *t* test.

puted membrane resistance ratios for the "K⁺ Ringer's" condition. Apical membrane specific conductance was clearly decreased after NaCl replacement ($G_a = 0.06 \pm 0.01$ mS/ μ F). Results for the basolateral membrane specific conductance were more variable. For example, a significant increase was obtained only for the lumped model. The LIS-distributed model and crypt-distributed model results showed no significant change from controls.

Mean values for distributed resistances were larger and more variable for this condition but were not significantly different from the control (NaCl Ringer's) condition. R_a/R_b values computed for the impedance-determined conductances were increased by approximately tenfold to a mean value of 51 ± 6 . To determine the effects of a significant LIS path resistance, we next computed α , assuming R_p values obtained from the distributed model. Our calculations indicated that DC microelectrode measurements would underestimate the resistance ratio by an average of $34 \pm 4\%$ under these conditions, giving a mean value for α of only 26 ± 6 . This finding is in conflict with our previous work (Wills et al., 1979) which found an average α value of 8 ± 1 in microelectrode measurements in surface epithelial

cells. Consequently a discrepancy exists between the impedance-determined values of α and microelectrode measurements of this parameter in surface cells. This discrepancy cannot be explained by distributed resistance effects (see Discussion). For specific membrane conductances, $R_{a,\text{norm}}/R_{b,\text{norm}}$ was 51 ± 11 for the lumped model, 17 ± 5 , for the LIS model and 11 ± 4 for the crypt-distributed model.

Discussion

In this study we have measured the transepithelial impedance of the rabbit descending colon under control conditions and under two other conditions in which net Na⁺ transport was inhibited (i.e., by mucosal addition of the Na⁺ channel blocking agent amiloride and by removal of Na⁺ from the mucosal bath). In addition to reporting these measurements, we have evaluated the relative importance of distributed resistance effects in the determination of membrane conductances and capacitances. To achieve this assessment, we analyzed the impedance using three different models: a simple

"lumped" model and two morphologically-based distributed models (see below).

VALIDATION OF MEASUREMENTS

The use of transepithelial impedance measurements requires a number of considerations. For example, the current signal must be small enough to permit measurements within the linear I - V range of the epithelium, yet be large enough for an adequate signal-to-noise ratio. In the present study, these factors were not a problem since Thompson, Suzuki, and Schultz (1982a,b) have demonstrated that the I - V relationship of the colon is linear within the current and voltage ranges investigated. Moreover, the rabbit descending colon, unlike so-called "leaky" epithelia such as the gallbladder has a transcellular resistance that is comparable to the paracellular conductance (Wills et al., 1979). This property permits analysis of its impedance by transepithelial methods, as opposed to microelectrode methods.

Another consideration in the present study was the need for an independent estimate of paracellular conductance for analysis of the impedance data. The estimate that we used was derived using the ionophore nystatin. This method and the assumptions involved in estimating G_s were previously described by Wills et al. (1979). Briefly, the method assumes that the paracellular pathway is essentially nonselective for Na^+ , K^+ , and Cl^- . This assumption has been verified by equivalent circuit analysis of the epithelium (Wills et al., 1979) and radioisotopic flux determinations (McCabe, Smith & Sullivan, 1984). Nonetheless, it is conceivable that G_s might differ for the three experimental conditions. Therefore, we determined the sensitivity of membrane impedance parameters to variations in the magnitude of G_s . G_s values from different animals had a standard error (SEM) equal to approximately 12% of the mean value.

To maximize variability in G_s , we arbitrarily varied G_s for individual experiments by $\pm 25\%$, i.e. by two standard deviations for the pooled mean. Data were then refitted for each of the models. Two tissues were selected for this analysis: one tissue with a high membrane resistance ratio and one tissue with a low resistance ratio. The results indicated that G_b and C_b were affected by less than $\pm 3\%$ when G_s was decreased or increased by 25%. On the other hand, G_a and C_a were more sensitive to alterations in G_s . G_a varied $\pm 18\%$ and C_a was altered by $\pm 6\%$ when G_s was increased or decreased by 25%. For this reason, we believe that the estimates are reasonably robust against errors in the measurement of G_s .

EVALUATION OF DISTRIBUTED RESISTANCE EFFECTS

Previous studies of several epithelia including the rabbit urinary bladder (Clausen et al., 1979), gastric mucosa (Clausen, Machen & Diamond, 1983), *Necturus* gallbladder (Kottra & Frömler, 1984a,b) and frog cornea (Clausen, Marcus & Reinach, 1987) have demonstrated significant distributed effects of the basolateral membrane resistance along the lateral intercellular space. In other words, the impedance of these epithelia could not be accurately described by a simple equivalent circuit model which ignores lateral intercellular space resistance (see lumped model, Fig. 1A). Our results suggest that in contrast to other epithelia studied so far, the rabbit descending colon can be reasonably approximated by the lumped model. Nonetheless, use of the LIS-distributed model and crypt-distributed model produced improved fits to the data. Small but statistically significant differences were found for G_a and C_b for the LIS model compared to the lumped model, whereas C_a and G_b showed a slight but statistically significant difference for the crypt model. For these reasons, we conclude that distributed resistance effects are detectable in the rabbit descending colon but have negligible effects on membrane impedances during normal conditions and during amiloride inhibition of net Na^+ absorption.

In recent experiments using the frog skin, Nagel, Garcia-Diaz and Essig (1983) showed that under certain conditions microelectrode measurements of membrane resistance ratios can be affected by distributed resistance effects. Specifically, they found evidence for erroneously low measurements of R_a/R_b after amiloride addition, which they ascribed to a distributed resistance of the basolateral membrane resistance along the LIS. This observation was made only for tissues with relatively high paracellular conductances. Consequently, they speculated that the rabbit descending colon, which has a high paracellular conductance compared to the frog skin, might also have such distributed resistance effects. Moreover, they further proposed that such an artifact might account for the residual conductance in the apical membrane in the presence of amiloride as measured by other investigators (Wills et al., 1979; Thompson et al. 1982a,b). We have referred to this conductance as the "amiloride-insensitive" conductance (Wills, 1985).

The present results argue against distributed resistance effects as an explanation of the apical membrane "amiloride-insensitive" conductance. First of all, the lateral intercellular spaces between surface cells appear relatively wide in micrographs (c.f. Wills, 1984) so a low resistance for the lateral

space would be expected. More importantly, the resistance of the lateral space is nearly three times lower ($R_p = 28 \pm 8 \Omega \cdot \text{cm}^2$) than the basolateral membrane resistance ($\sim 78 \Omega \cdot \text{cm}^2$). Consequently, distributed resistance effects would not be expected to predominate for the zero frequency (DC) case.

Membrane resistance ratios calculated from impedance data before and after amiloride addition (see Tables 2 and 5), were in excellent agreement with α values previously reported for colonic surface cells from DC microelectrode experiments (Schultz et al., 1977; Wills et al., 1979; Thompson et al., 1982a,b). According to the calculations of α in Table 5, microelectrode measurements would be decreased by 15% if the distributed resistance effects were localized to the LIS. This difference is too small to detect, given the variability between tissues. In any event, LIS-distributed effects are clearly too small to account for the observation of a significant apical membrane conductance in the presence of amiloride. Therefore, impedance measurements have provided independent evidence for an "amiloride-insensitive" conductance in these cells.

Although distributed resistance effects appear to be relatively small for control or amiloride conditions, this factor can become physiologically important for any condition that potentially causes cell swelling, constriction of the LIS, or otherwise increases R_{LIS} . For this reason, we also assessed the extent of distributed resistance effects for an additional condition, i.e., replacement of Na and Cl in the mucosal solution by potassium and sulfate or gluconate.

In this condition, large discrepancies were found between impedance estimates of R_a/R_b and previous microelectrode measurements of α in surface cells (mean $R_a/R_b = 51 \pm 6$; $\alpha = 8 \pm 1$, Wills et al., 1979). As indicated by the calculated α values in Table 7, this discrepancy cannot be accounted for by distributed resistance effects. Alternatively, we can "correct" the previous microelectrode measurement for the amount of underestimation (34%). Performing this "correction," we obtain an R_a/R_b value for surface cells equal to 10.7. This is less than a quarter of the value shown for R_a/R_b in Table 7. Since significant microelectrode impalement damage can be ruled out (see Lewis, & Wills & Eaton, 1979), we conclude that cells other than surface cells (i.e., crypt cells) must be responsible for this result. Note that the disparity is even worse with respect to the crypt-distributed model as this model predicts a slight (2%) overestimation of R_a/R_b by microelectrode measurements of α .

In summary, distributed resistance effects are

significant when Na and Cl are replaced in the mucosal bathing solution. For LIS-distributed effects, microelectrode estimates of α are expected to underestimate the "true" R_a/R_b by 34%. Crypt-distributed effects on α would produce only a slight overestimate (2%) of the "true" R_a/R_b . However, most importantly, all three models produce R_a/R_b estimates much larger than that measured in surface cells. Therefore, it is clear that surface cells differ from the rest of the epithelium in their conductance properties.

COMPARISON TO OTHER EPITHELIA

Because frequency domain methods provide estimates of both membrane capacitance and conductance, it is now possible to compare apical and basolateral membrane areas and area normalized conductances for the colon with various other epithelia that have been studied using this technique. Table 8 is a summary of available impedance results from both tight and leaky epithelia bathed in NaCl Ringer's solutions. With respect to the magnitude of its apical membrane capacitance, the colon is second only to gastric mucosa. Since 1 μF of membrane capacitance is approximately equal to 1 cm^2 of membrane area, this capacitance indicates a large apical membrane surface area for the colon, approximately 20 cm^2 . One likely explanation for this large area is the presence of microvilli in this membrane. The basolateral membrane, in contrast, had a capacitance approximately one half this value, comparable to C_b for the rabbit urinary bladder.

Because amiloride-sensitive Na^+ transport in the colon is approximately 20–50 times larger than in the urinary bladder, it is useful to compare the normalized apical membrane conductances of these two epithelia. As shown in Table 8, total apical membrane conductance is larger for the colon than for the urinary bladder (0.17 and 0.08 $\text{mS}/\mu\text{F}$, respectively). Similarly, the amiloride-insensitive conductance of this membrane is larger in the colon (0.080 $\text{mS}/\mu\text{F}$) than that reported for the rabbit urinary bladder membrane (0.012 $\text{mS}/\mu\text{F}$). However, when the amiloride-insensitive component is subtracted from the total apical membrane conductance, the two tissues appear to have comparable amiloride-sensitive Na^+ conductances. Consequently, the larger rate of Na^+ transport across the colon appears to be due to its larger apical membrane surface area.

A striking difference between the colon and other epithelia is its large basolateral membrane conductance. When normalized to area, this con-

Table 8. Comparison of epithelial impedances estimated using distributed resistance models

Tissue	G_a (mS/cm ²)	C_a (μ F/cm ²)	G_{bl} (mS/cm ²)	C_{bl} (μ F/cm ²)	R_{LIS}	R_{crypt}	G_{a-norm} (mS/cm ²)	$G_{bl-norm}$ (μ F/cm ²)	Reference
Rabbit descending colon	3.5	21	12.7	11	28	—	0.18	1.16	(This study)
	3.7	22	12.8	11	—	22	0.16	1.19	(This study)
Rabbit urinary bladder	0.2	2	1.0	9	130	—	0.08	0.12	Clausen et al. (1979)
Frog stomach (nonsecreting)	6.7	200	24.4	99	—	24	0.004	0.25	Clausen et al. (1983)
Frog cornea	1.9	3	1.1	94	331	—	0.17	0.01	Clausen et al. (1986)
<i>Necturus</i> gallbladder	0.3	5	4.4	27	36	—	0.06	0.02	Kottra and Frömler (1984a,b)

ductance appears to be an order of magnitude larger than that of any epithelium studied so far.

AMILORIDE EFFECTS ON MEMBRANE PROPERTIES

Amiloride is known to block Na^+ channels in the apical membrane of the rabbit descending colon (Zeiske, Wills & Van Driessche, 1982). In agreement with these findings, the present study found that mucosal addition of amiloride decreased apical membrane conductance. In addition, there was an 18% decrease in apical membrane capacitance and a 13% decrease in basolateral membrane conductance. In previous experiments, G_b was found to be largely a potassium conductance (Wills et al., 1979). The basolateral membrane potential and intracellular potassium activities showed little change after mucosal amiloride addition (Wills, Clausen & Clauss, 1987). Consequently, it is likely that the decrease in G_b reflects a true change in the permeability of this membrane. This finding differs from previous results, which were consistent with a single-site action of amiloride, i.e., a blockage of the apical membrane Na^+ conductance. For example, transepithelial conductance linearly decreased with the decrease in short-circuit current (Schultz et al., 1977; Wills et al., 1979; Thompson et al., 1982a,b).

We note that in the present study, measurements were typically made after 2–5 min following full effect of the drug, whereas in our previous microelectrode experiments, measurements were made during amiloride addition until maximum drug action occurred (i.e., 1–4 min earlier than impedance measurements). Consequently, we may have missed the decrease in G_{bl} in our previous experiments. Davis and Finn (1982) have reported reduc-

tions in basolateral membrane conductance in toad urinary bladder after mucosal amiloride addition to inhibit net Na^+ transport. We should note that it is also conceivable that this effect might be too small to detect with microelectrode techniques or, alternatively, might be mediated by cells that were not impaled by microelectrodes in our previous study (i.e., crypt cells). The mechanism of this decrease clearly requires further study.

A small unexplained decrease also occurred in the apical membrane capacitance after amiloride addition. To assess the possible source of this decrease, we performed preliminary computer simulations of transepithelial impedance before and after amiloride addition using an equivalent circuit containing two electrically-uncoupled cell types (one amiloride-sensitive and the other amiloride-insensitive). The resulting impedance data were then fitted using the lumped model shown in Fig. 1. The results indicated that the presence of two electrically uncoupled cell types could not explain the decrease in C_a . We note that apical membrane area changes due to vesicle fusion have been proposed for rabbit urinary bladder (Lewis & deMoura, 1984) and toad bladder (Stetson, Lewis, Alles & Wade, 1981). However, vesicle fusion has not been reported for the Na^+ -transporting cells of the colon. It was beyond the scope of the present study to identify the source of this capacitance decrease.

As noted in the results for the amiloride experiments, E_{Na} and R_s values estimated by DC equivalent circuit methods were highly variable. This variability could suggest that more than one circuit element is altered by amiloride. In contrast to our earlier studies, nonlinear effects of amiloride were observed in a few instances. Therefore, the effects of amiloride on the colon may be more complex than previously believed.

ALTERATIONS OF MEMBRANE PROPERTIES BY MUCOSAL Na^+ AND Cl^-

Inhibition of Na^+ transport by replacement of Na^+ and Cl^- by potassium and gluconate or sulfate led to a decrease in apical membrane conductance and capacitance similar to that produced by amiloride. As in the case of amiloride, this apparent decrease in apical membrane capacitance was unexpected and we can offer no explanation at this time. When apical membrane conductance is normalized to membrane capacitance, it is apparent that an appreciable apical membrane conductance is present even in the absence of mucosal Na^+ and Cl^- .

In contrast to the effects of amiloride, basolateral membrane conductance and capacitance were greatly increased. When this increase in conductance was normalized to membrane capacitance, however, the increase in specific membrane conductance was not significant for the distributed models. It is tempting to speculate that basolateral membrane area is increased in the presence of "K⁺ Ringer's" solutions and that the newly inserted membrane has similar conductance properties. However, verification of this conclusion will require morphometric analysis of this epithelium.

SIGNIFICANCE OF THE APICAL MEMBRANE AMILORIDE-SENSITIVE CONDUCTANCE

Because the paracellular conductance is nearly equal to the transcellular conductance of the rabbit descending colon, the apical membrane is electrically coupled to the basolateral membrane such that changes in the apical membrane potential are attenuated. This factor hinders direct assessment of the ionic selectivity of the apical membrane amiloride-insensitive conductance. Nonetheless, the results of DC equivalent circuit analysis and intracellular ion activity measurements (Wills, 1985) indicate that this conductance is largely due to potassium. We can estimate a minimum magnitude for this conductance by using data from previous microelectrode studies and new information from the present study concerning distributed resistances. More specifically, we can "correct" α values from previous experiments (Wills et al., 1979; Thompson et al., 1982a,b) for attenuation caused by distributed resistance effects and use this "corrected" estimate to determine the apical membrane conductance in the presence of amiloride. For the LIS-distributed model, the "corrected" R_a/R_b is 10.7. Assuming a basolateral resistance of $\sim 160 \Omega \cdot \text{cm}^2$ (Wills et al., 1979) or $\sim 100 \Omega \cdot \text{cm}^2$ (Thompson et al., 1982a,b), the apical membrane amiloride-insensitive conduc-

tance in surface cells is approximately $0.6\text{--}0.9 \text{ mS/cm}^2$ or ($R_a = 1.1\text{--}1.7 \text{ k}\Omega \cdot \text{cm}^2$). In the present study, a decrease was noted for the basolateral membrane conductance after amiloride. If this decrease is localized to surface cells, then the above conductance estimate would be similarly decreased by 25% to $\sim 0.5\text{--}0.7 \text{ mS/cm}^2$. Again, this is a minimum estimate for the amiloride-insensitive conductance in the apical membrane of surface cells.

Wills (1984) has proposed that potassium secretion by the colon occurs via a conductive mechanism. Therefore, it is interesting to compare the above estimate of amiloride-insensitive conductance for surface cells to the total apical membrane conductance measured using impedance analysis for the "K⁺ Ringer's" condition (i.e., the conductance for both surface and crypt cells). Using the constant field conductance equation (see Schultz, 1984, pg. 119), measurements of the apical membrane potential under these conditions (-32 mV cell interior negative; Wills et al., 1979 and *unpublished*), and impedance-determined values for apical membrane conductance, we estimated the apical membrane potassium permeability (P_K) as approximately $1.7 \times 10^{-7} \text{ cm/sec}$. This calculation assumes that the apical membrane potential is similar for crypt and surface cells under these conditions (mucosal $[K^+] = 143 \text{ mM}$). If true, the apical membrane potassium conductance for the NaCl Ringer's condition (mucosal $[K^+] 7\text{mM}$) would be 0.013 mS/cm^2 , corresponding to a resistance of $78 \text{ k}\Omega \cdot \text{cm}^2$. The large discrepancy between this value and the amiloride-insensitive conductance suggests that: (1) either P_K is not constant and is reduced in the K⁺ Ringer's condition or (2) that the apical membrane potential in crypt cells is different from that in surface cells. Further evaluation of this issue will require membrane potential measurements in crypt cells.

CONCLUSIONS

In summary, our analysis of the impedance properties of the rabbit descending colon indicates that distributed resistance effects can be detected but have negligible effects on impedance estimates of membrane parameters. Distributed resistance effects due to the LIS resistance would be expected to decrease microelectrode estimates of membrane resistance ratios by 12–15% for control and amiloride conditions and by 34% when potassium sulfate or potassium gluconate Ringer's solutions are used as the mucosal bathing solution. The results support the hypothesis of an apical membrane conductance in surface cells that is amiloride-insensi-

tive and that is not due to sodium or chloride. Further experiments are needed to resolve the impedance properties of crypts and surface cells in this epithelium.

References

Boulpaep, E.L., Sackin, H. 1980. Electrical analysis of intraepithelial barriers. In: *Current Topics in Membranes and Transport: Cellular Mechanisms of Renal Tubular Ion Transport*. E.L. Boulpaep, editor. pp. 169–197. Academic, New York.

Clausen, C., Fernandez, J.M. 1981. A low-cost method for rapid transfer function measurements with direct application to biological impedance analysis. *Pfluegers Arch.* **390**:290–295.

Clausen, C., Lewis, S.A., Diamond, J.M. 1979. Impedance analysis of a tight epithelium using a distributed resistance model. *Biophys. J.* **26**:291–317.

Clausen, C., Machen, T.E., Diamond, J.M. 1983. Use of A.C. impedance analysis to study membrane changes related to acid secretion in amphibian gastric mucosa. *Biophys. J.* **41**:167–178.

Clausen, C., Reinach, P.S., Marcus, D.C. 1986. Membrane transport parameters in frog corneal epithelium measured using impedance analysis techniques. *J. Membrane Biol.* **91**:213–255.

Cole, K.S. 1972. *Membranes, Ions, and Impulses*. p.12. University of California Press, Berkeley.

Davis, C.W., Finn, A.L. 1982. Sodium transport inhibition by amiloride reduces basolateral membrane potassium conductance in tight epithelia. *Science* **216**:525–527.

Frizzell, R.A., Koch, M.J., Schultz, S.G. 1976. Ion transport by rabbit colon: I. Active and passive components. *J. Membrane Biol.* **27**:297–316.

Hamilton, W.C. 1964. *Statistics in Physical Science*. pp. 69–88. Ronald, New York.

Kottra, G., Frömter, E. 1984a. Rapid determination of intraepithelial resistance barriers by alternating current spectroscopy. *Pfluegers Arch.* **402**:409–420.

Kottra, G., Frömter, E. 1984b. Rapid determination of intraepithelial resistance barriers by alternating current spectroscopy: II. Test of model circuits and quantification of results. *Pfluegers Arch.* **402**:421–432.

Lewis, S.A., Moura, J.L.C. de 1984. Apical membrane area of rabbit urinary bladder increases by fusion of intracellular vesicles: An Electrophysiological study. *J. Membrane Biol.* **82**:123–136.

Lewis, S.A., Wills, N.K. 1982. Electrical properties of the rabbit urinary bladder assessed using gramicidin D. *J. Membrane Biol.* **67**:45–53.

Lewis, S.A., Wills, N.K., Eaton, D.C. 1979. Membrane selectivity and ion activities of mammalian tight epithelia. *Curr. Top. Membr. Transp.* **13**:199–212.

McCabe, R.D., Cooke, H.J., Sullivan, L.P. 1982. Potassium transport by rabbit descending colon. *Am. J. Physiol.* **242**:C81–C86.

McCabe, R.D., Smith, P.L., Sullivan, L.P. 1984. Ion transport by rabbit descending colon: Mechanisms of transepithelial potassium transport. *Am. J. Physiol.* **246**:6594–6602.

Nagel, W., Garcia-Diaz, J.F., Essig, A. 1983. Contribution of junctional conductance to the cellular voltage-divider ratio in frog skins. *Pfluegers Arch.* **399**:336–341.

Schultz, S.G., Frizzell, R.A., Nellans, H.N. 1977. Active sodium transport and the electrophysiology of rabbit colon. *J. Membrane Biol.* **33**:351–384.

Stetson, D.L., Lewis, S.A., Alles, W., Wade, J.B. 1982. Evaluation by capacitance measurements of antidiuretic hormone induced membrane area changes in toad bladder. *Biochim. Biophys. Acta* **684**:267–274.

Thompson, S.M., Suzuki, Y., Schultz, S.G. 1982a. The electrophysiology of rabbit descending colon: I. Instantaneous transepithelial current-voltage relations and the current-voltage relations of the Na⁺-entry mechanism. *J. Membrane Biol.* **66**:41–54.

Thompson, S.M., Suzuki, Y., Schultz, S.G. 1982b. The electrophysiology of rabbit descending colon: II. Current-voltage relations of the apical membrane, the basolateral membrane, and the parallel pathways. *J. Membrane Biol.* **66**:55–61.

Valdiosera, R., Clausen, C., Eisenberg, R.S. 1974. Circuit models of the passive electrical properties of frog skeletal muscle fibers. *J. Gen. Physiol.* **63**:432–459.

Welsh, M.J., Smith, P.L., Fromm, M., Frizzell, R.A. 1982. Crypts are the site of intestinal fluid and electrolyte secretion. *Science* **218**:1219–1221.

Wills, N.K. 1981. Antibiotics as tools for studying the electrical properties of tight epithelia. *Fed. Proc.* **40**:2202–2205.

Wills, N.K. 1984. Mechanisms of ion transport by the mammalian colon revealed by frequency domain analysis techniques. *Curr. Top. Membr. Transp.* **20**:61–85.

Wills, N.K. 1985. Apical membrane potassium and chloride permeabilities in surface cells of rabbit descending colon epithelium. *J. Physiol. (London)* **358**:433–445.

Wills, N.K., Alles, W.P., Sandle, G.I., Binder, H.J. 1984. Apical membrane properties and amiloride binding kinetics of the human descending colon. *Am. J. Physiol.* **247**:G749–G757.

Wills, N.K., Biagi, B. 1982. Active potassium transport by rabbit descending colon epithelium. *J. Membrane Biol.* **64**:195–203.

Wills, N.K., Clausen, C., Clauss, W. 1987. Electrophysiology of active potassium transport across the mammalian colon. *Curr. Topics Membr. Transp.* (in press).

Wills, N.K., Lewis, S.A., Eaton, D.C. 1979. Active and passive properties of rabbit descending colon: A microelectrode and nystatin study. *J. Membrane Biol.* **45**:81–108.

Zeiske, W., Wills, N.K., Van Driessche, W. 1982. Na⁺ channels and amiloride-induced noise in the mammalian colon epithelium. *Biochim. Biophys. Acta* **688**:201–210.

Received 9 April 1986; revised 8 September 1986